VOLUME 1
PERFORMANCE FLIGHT TESTING

CHAPTER 14

AERODYNAMIC MODELING

JANUARY 1996

USAF TEST PILOT SCHOOL
EDWARDS AIR FORCE BASE, CALIFORNIA

This textbook, *Aerodynamic Modeling*, was written in July of 1992 to provide USAF Test Pilot School students with an understanding of stabilized, quasisteady-state, and dynamic aerodynamic modeling performance flight test techniques.

Author:

Gregory L. Beeker

GREGORY L. BEEKER
Captain, USAF
Chief Performance Engineer

This textbook has been reviewed and is approved for publication:
10 Dec 1993

Richard L. Bennett

RICHARD L. BENNETT
Major, USAF
Chief, Performance Branch

James M Payne

JAMES M. PAYNE
Lieutenant Colonel, USAF
Director of Student Training

TABLE OF CONTENTS

(This page intentionally left blank)

14.1 INTRODUCTION

Over the past 20 years, more and more aircraft performance testing is being dedicated to the validation of aerodynamic and propulsion system models for use in performance prediction routines. Since it has always been impractical to test an aircraft at every flight condition, mathematical aircraft models have served as tools which allowed us to "extrapolate" beyond the actual test points in the production of flight manuals and other performance documentation. The development of better aircraft models not only provides more confidence in the extrapolation of test data, but reduces the amount of performance flight testing actually required.

The purpose of this course is to provide an understanding of the role of aerodynamic models in aircraft performance predictions and to introduce the stabilized, quasi-steady-state, and dynamic flight test methods for building these models.

14.2 AERODYNAMIC MODELS

An aircraft aerodynamic model consists of a set of drag polars and a corresponding set of lift curves (Reference 1). Drag polars define the relationship between the airframe lift coefficient, C_L, and drag coefficient, C_D, while lift curves define the relationship between the airframe lift coefficient and angle of attack, α. For each aircraft configuration and loading combination, drag polars and lift curves are dependent on Mach number, M, center of gravity location, cg, dynamic trim drag, Reynold's number, R_e, and structural flexing. Of these, Mach number, center of gravity location, and Reynold's number (presented in the form of an altitude effect) generally provide the most significant effects. Thus, for the drag polar, we will assume

$$C_D = f\ (C_L, M, R_e \text{ or } H_c, cg) \tag{14.1}$$

And for the lift curve;

$$\alpha = f\ (C_L, M, R_e \text{ or } H_c, cg) \tag{14.2}$$

Generally, drag polar and lift curve data for a particular configuration and loading are presented as functions of Mach number at a given altitude and cg, as shown in Figures 14.1 and 14.2 for the F-16B aircraft. Notice that as the Mach number increases, the drag polar shifts in the direction of increasing drag coefficient, as expected, due to flow separation and the formation of shock waves.

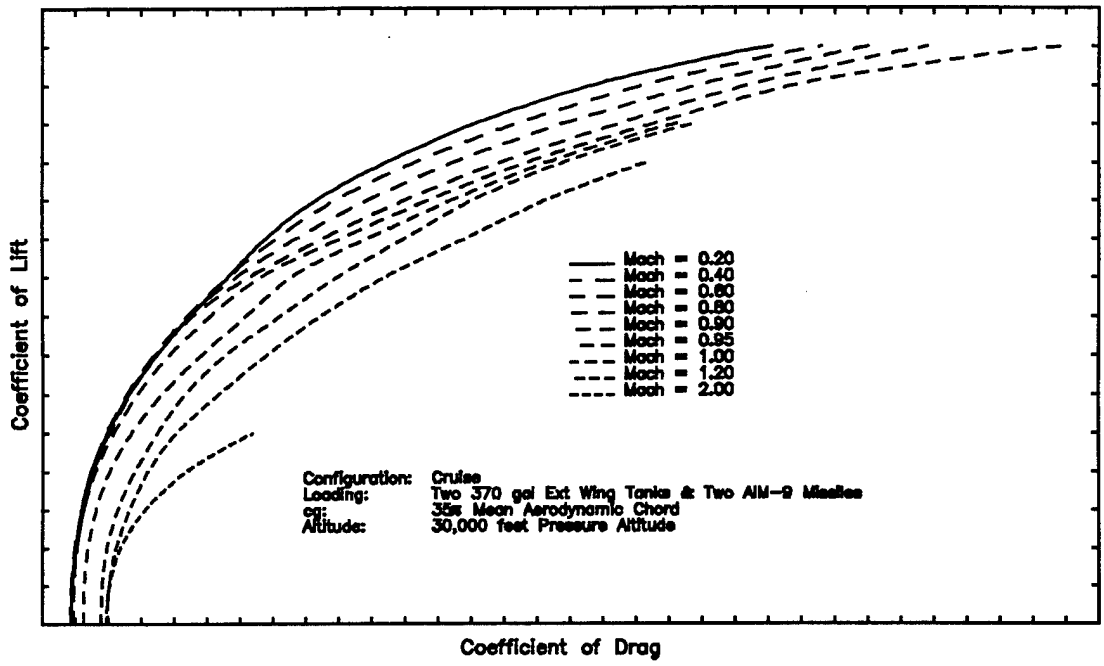

Figure 14.1 F-16B Drag Polars at Constant Altitude and Center of Gravity

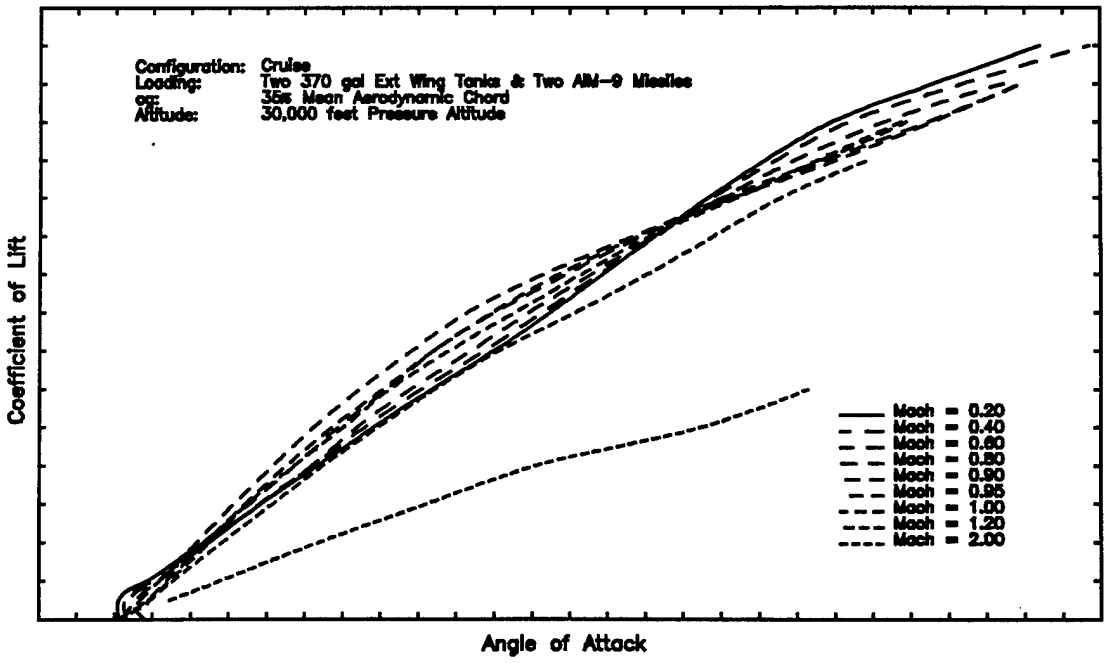

Figure 14.2 F-16B Lift Curves at Constant Altitude and Center of Gravity

To better understand the significance of altitude and cg variation on aircraft aerodynamic characteristics, consider Figures 14.3-14.6. These figures show that the F-16B drag polars and lift curves are more dependent on cg than altitude. Only at altitudes below 20,000 ft pressure altitude (PA) with Mach numbers above 0.9 does the lift curve become moderately affected by altitude changes. Other aircraft may show different results. For example, while the F-15B aircraft drag polars (Figure 14.7) are like that of the F-16B - more dependent on cg than altitude - the F-15B lift curves (Figure 14.8) are more dependent on altitude.

An aircraft aerodynamic model is, in general, first developed using data obtained during wind tunnel testing. This initial model can later be corrected using flight test data. Once an aerodynamic model is developed, it can be used in conjunction with an accurate engine model to predict the standard day or test day performance of an aircraft at any flight condition modeled. The predictions can then be spot checked using data from maneuver and cruise performance flight tests.

14.3 FLIGHT TEST METHODS FOR DETERMINING AERODYNAMIC CHARACTERISTICS

The characterization of lift and drag of an aircraft can be performed using any of a variety of flight test methods. The aircraft type, availability of a valid engine model, and desired accuracy are all factors which must be considered when determining the best aerodynamic modeling flight test method for a given test program. Data are generally collected for a particular Mach number at various load factors (ie C_L values) in order to develop the constant Mach curves which make up the drag polars and lift curves. However, for low subsonic speed aircraft, the Mach number effects are negligible. Therefore, the aerodynamic characteristics for a given aircraft configuration and loading can be modeled with a single drag polar and lift curve at a particular altitude and cg. This allows data collected at a variety of speeds to be used in the development of this model.

14.3.1 AERODYNAMIC CHARACTERIZATION USING ENGINE MODELS

In the past, the construction of an accurate thrust deck was the limiting factor in performance testing. As a result, performance data were collected without the requirement to accurately measure installed thrust. However, today thrust can be modeled very accurately. In fact, on the X-29 project, real-time thrust values were obtained to within 3-5% using 8 different telemetered pressure measurements.

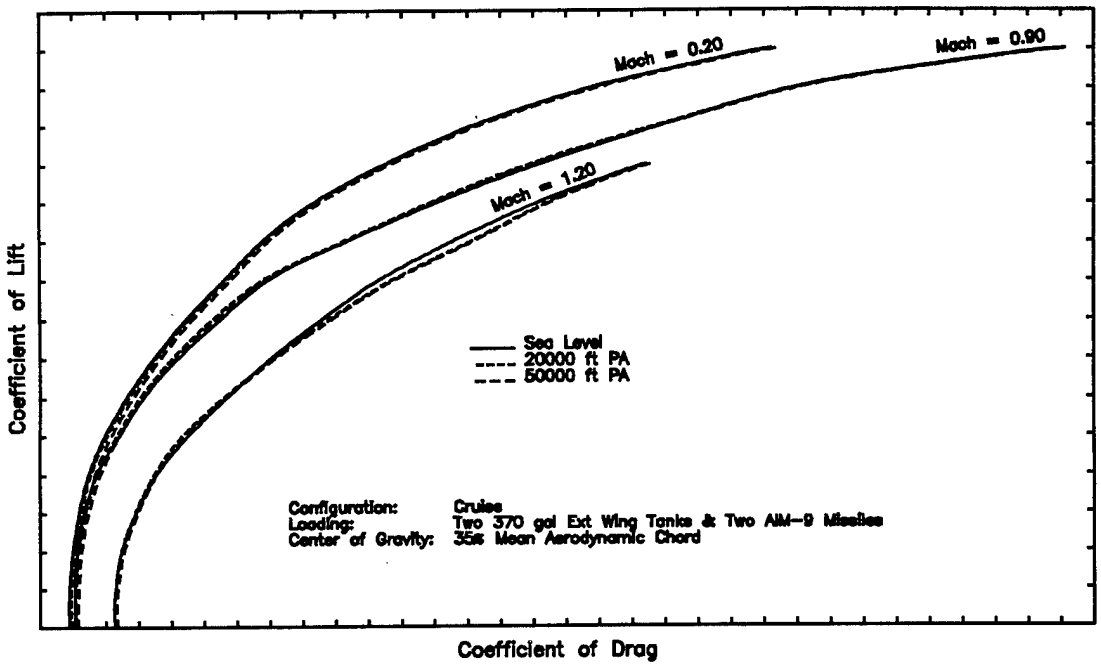

Figure 14.3 F-16B Drag Polar Altitude and Mach Number Effects

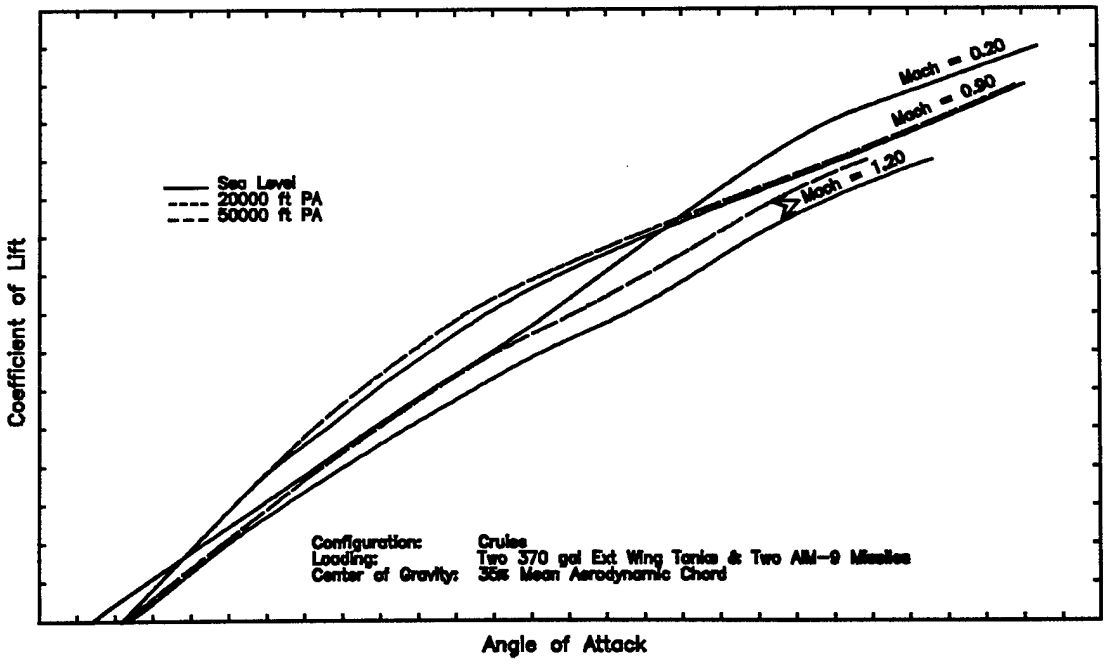

Figure 14.4 F-16B Lift Curve Altitude and Mach Number Effects

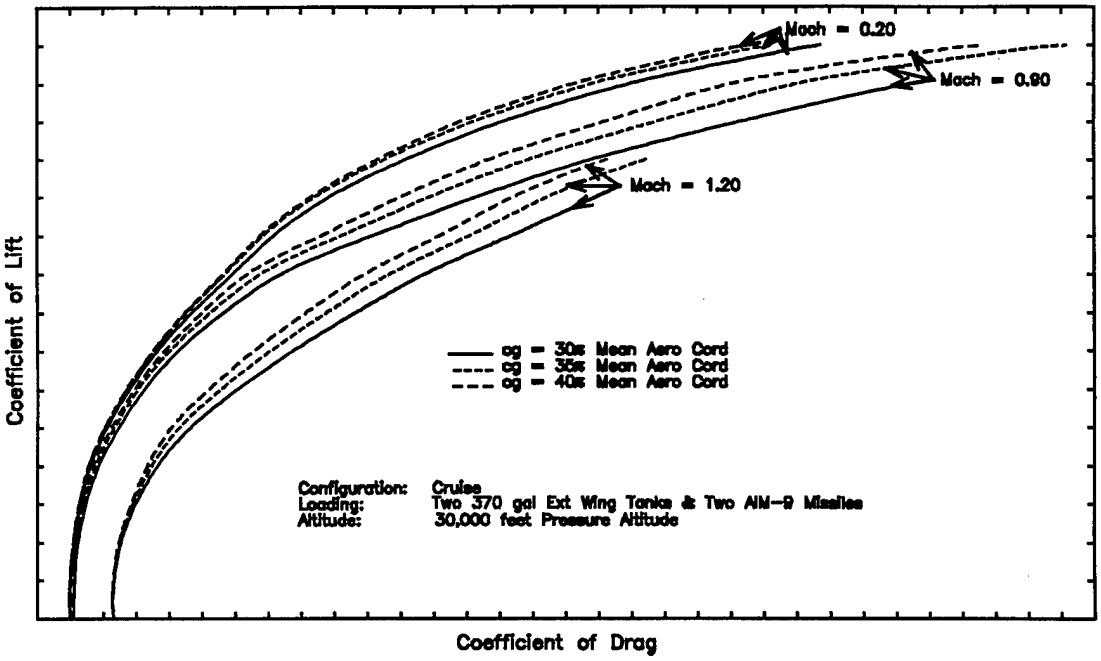

Figure 14.5 F-16B Drag Polar Center of Gravity and Mach Number Effects

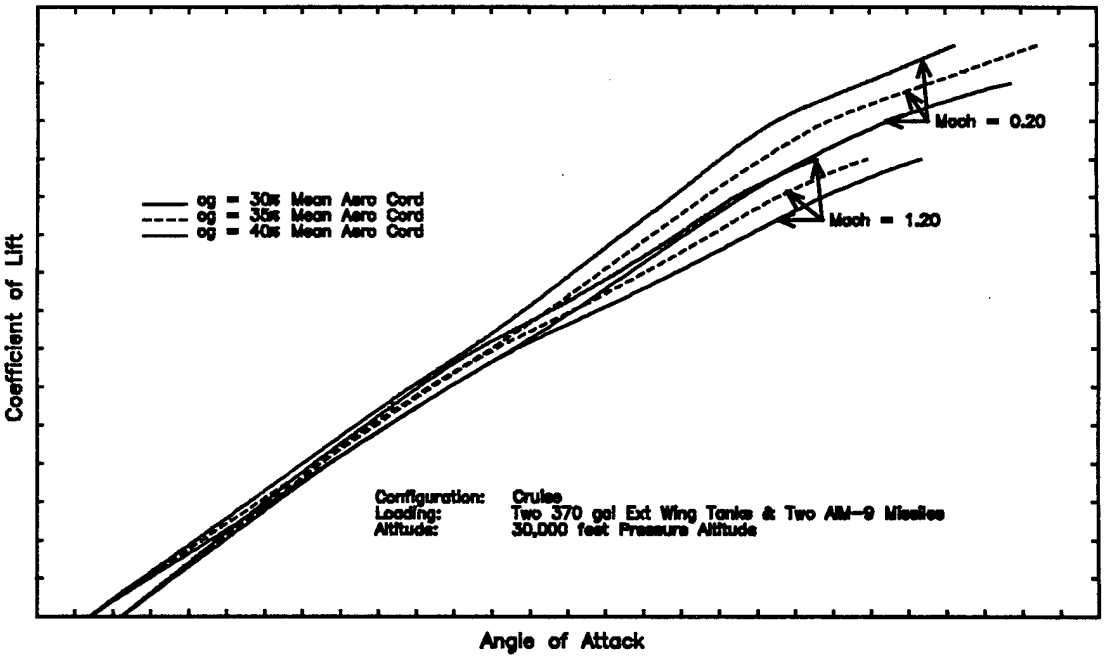

Figure 14.6 F-16B Lift Curve Center of Gravity and Mach Number Effects

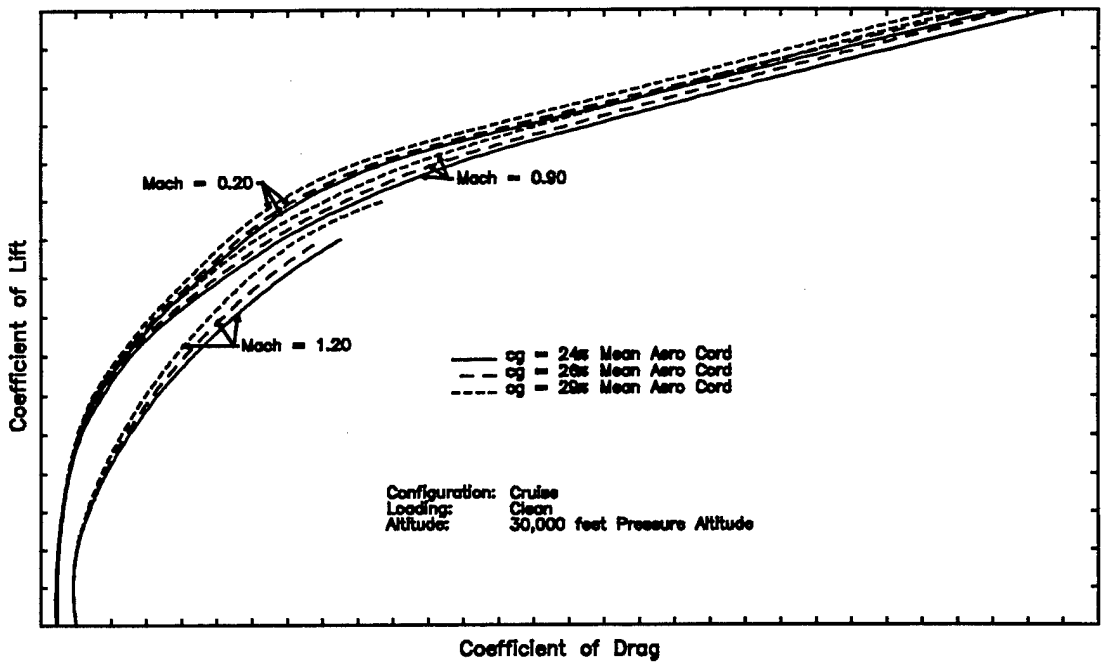

Figure 14.7 F-15B Drag Polar Center of Gravity and Mach Number Effects

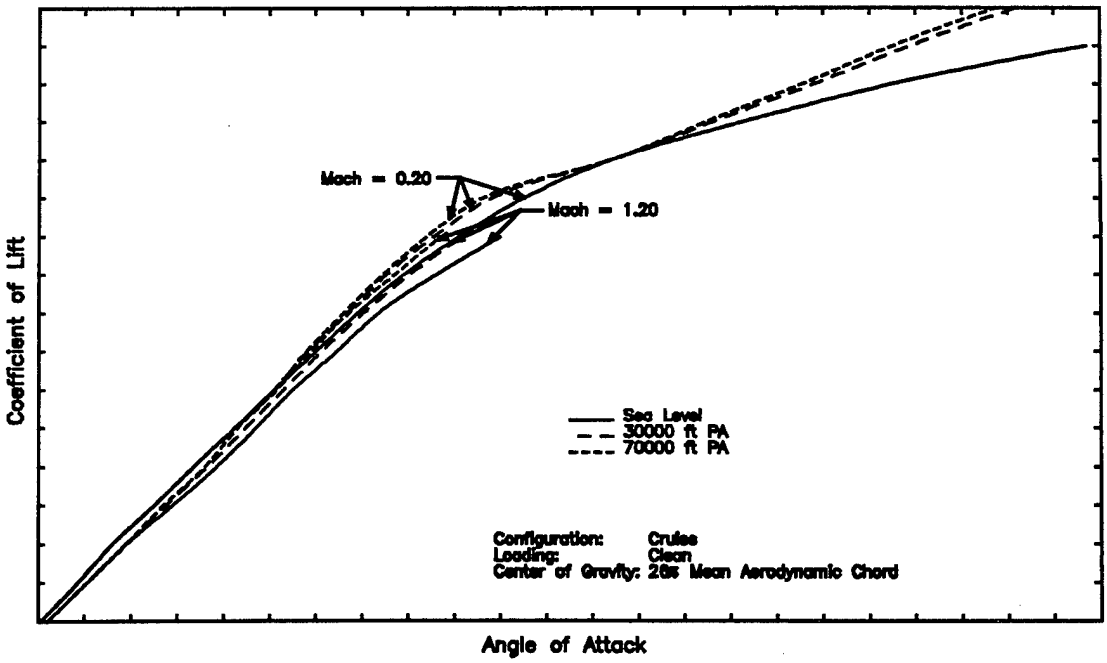

Figure 14.8 F-15B Lift Curve Altitude and Mach Number Effects

The aerodynamic modeling methods presented for determining lift and drag characteristics using contractor engine models can be broken into three categories: stabilized, quasisteady-state, and dynamic methods. Stabilized methods include constant altitude and descending turn maneuvers which allow data collection during stabilized test points at various load factors. Quasisteady-state methods include level accelerations and decelerations performed to take advantage of the variation in lift coefficient with airspeed. They are primarily used for slow speed aircraft whose aerodynamic characteristics are not significantly influenced by Mach number effects. Finally, dynamic methods include roller coaster, wind-up turn, and split-S maneuvers to obtain data at a wide range of load factors. The stabilized methods provide limited, but reliable, data for limited instrumentation, and can be used to validate the results of other methods. The significance of dynamic performance methods is the ability to accumulate large amounts of performance data from a single maneuver. Rather than accomplish a large number of quasisteady-state or stabilized test points, a smaller number of dynamic maneuvers may be flown. Figures 14.9-14.16 illustrate this concept, comparing data collected on a series of stable points with that collected during a single roller coaster and split-S maneuver.

14.3.1.1 STABILIZED METHODS

Stabilized methods can provide data for load factors from 1-g to maximum g (aircraft lift or structural limit) at a given altitude. The aircraft is stabilized at a given Mach number, altitude, load factor, and power setting, with sideslip angle held to zero. Once stabilized, the aircraft is maintained stable for approximately 10 seconds to allow for data collection at the desired altitude. The disadvantages of these methods are that each maneuver provides only a single point of the drag polar and lift curve and takes several minutes to set up. The advantage is that only limited instrumentation is needed for data collection. Data required for stabilized methods include calibrated airspeed, pressure altitude, ambient temperature, climb rate, pitch angle, roll angle, angle of attack (if available), and the engine parameters necessary for thrust determination (C-23: Output shaft torque, τ_s, and propeller speed, N_p; C-141: engine pressure ratio, EPR; F-15, F-16, or T-38: engine core speed, N_2).

14.3.1.1.1 CONSTANT ALTITUDE

This method allows data to be collected during constant altitude flight, thereby removing the possibility of altitude (Reynold's Number) or structural flexing effects. The aircraft is stabilized at the test Mach number, altitude, and load factor. Throttle

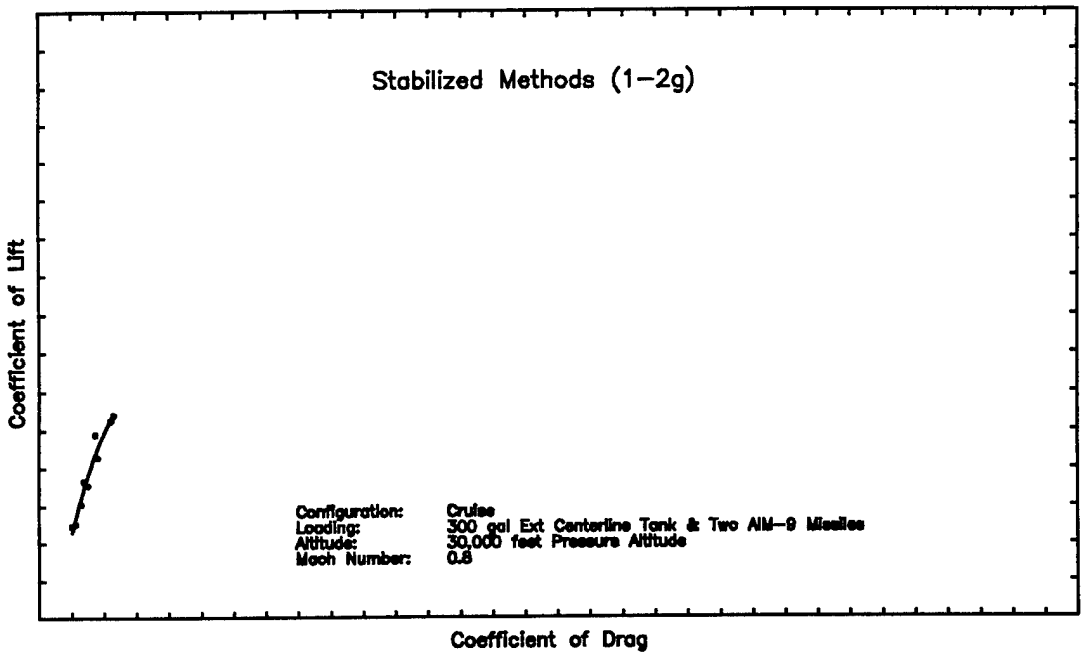

Figure 14.9 F-16B Drag Data obtained from Stabilized Methods

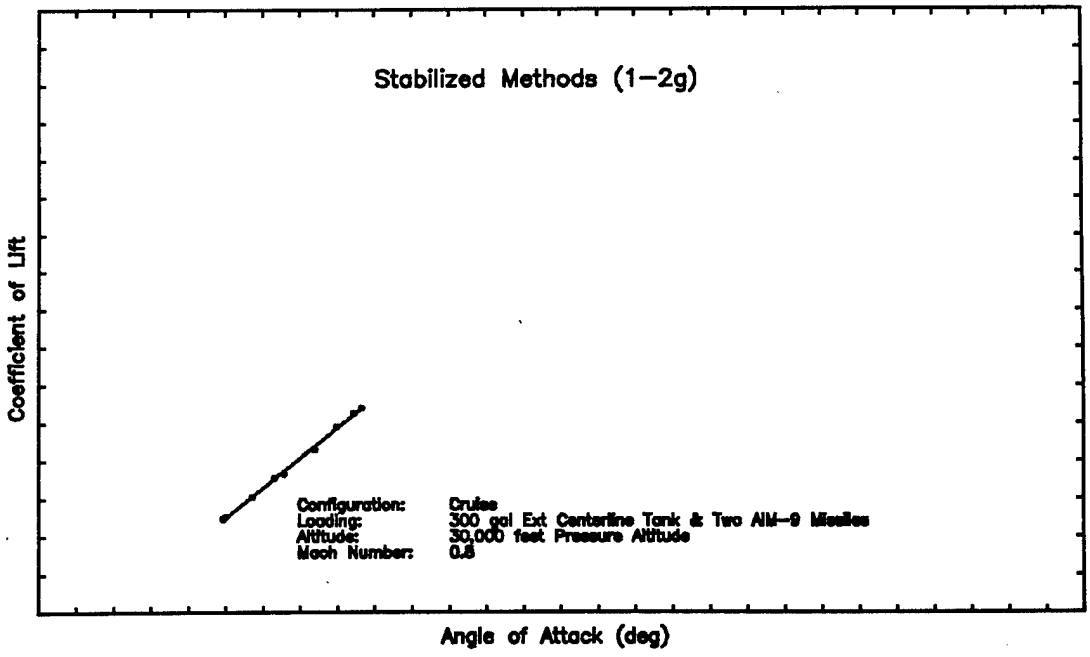

Figure 14.10 F-16B Lift Data obtained from Stabilized Methods

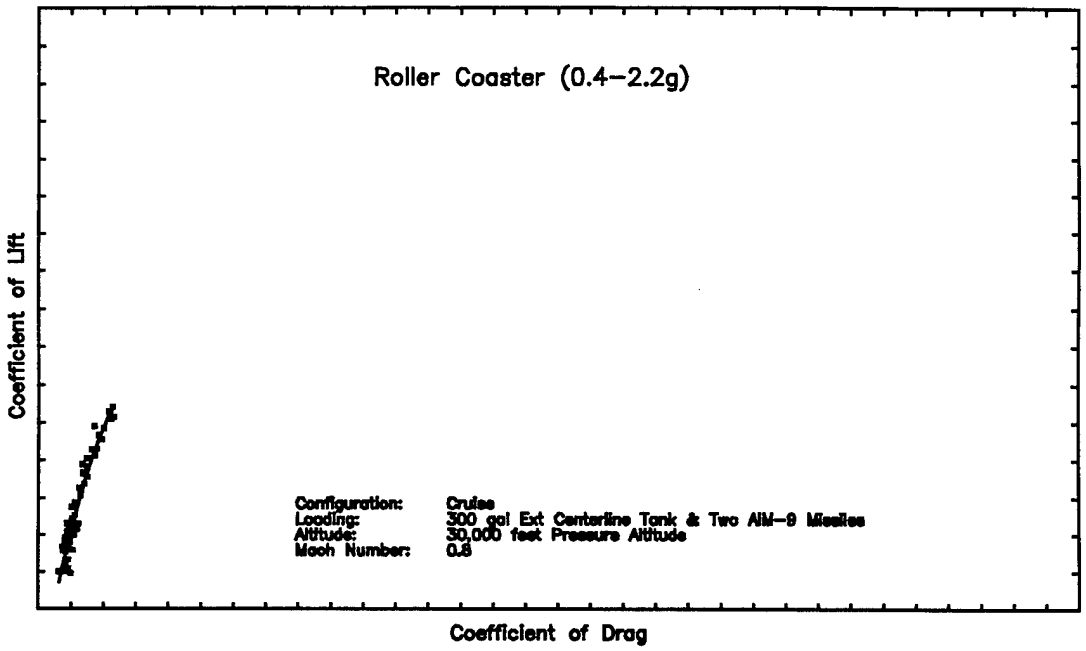

Figure 14.11 F-16B Drag Data obtained from a Roller Coaster Maneuver

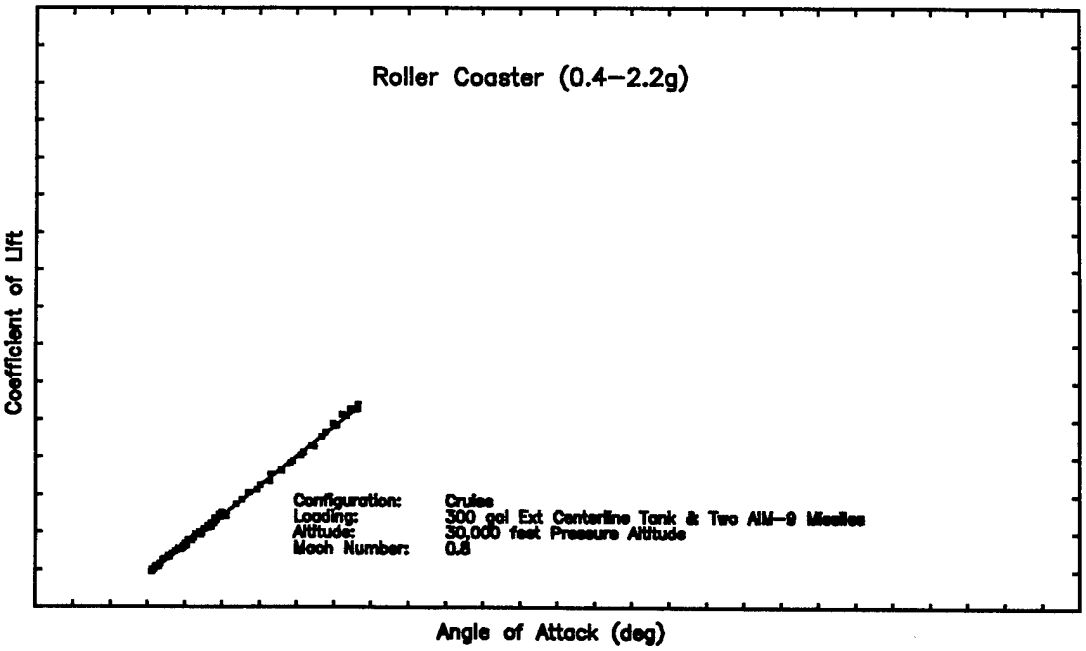

Figure 14.12 F-16B Lift Data obtained from a Roller Coaster Maneuver

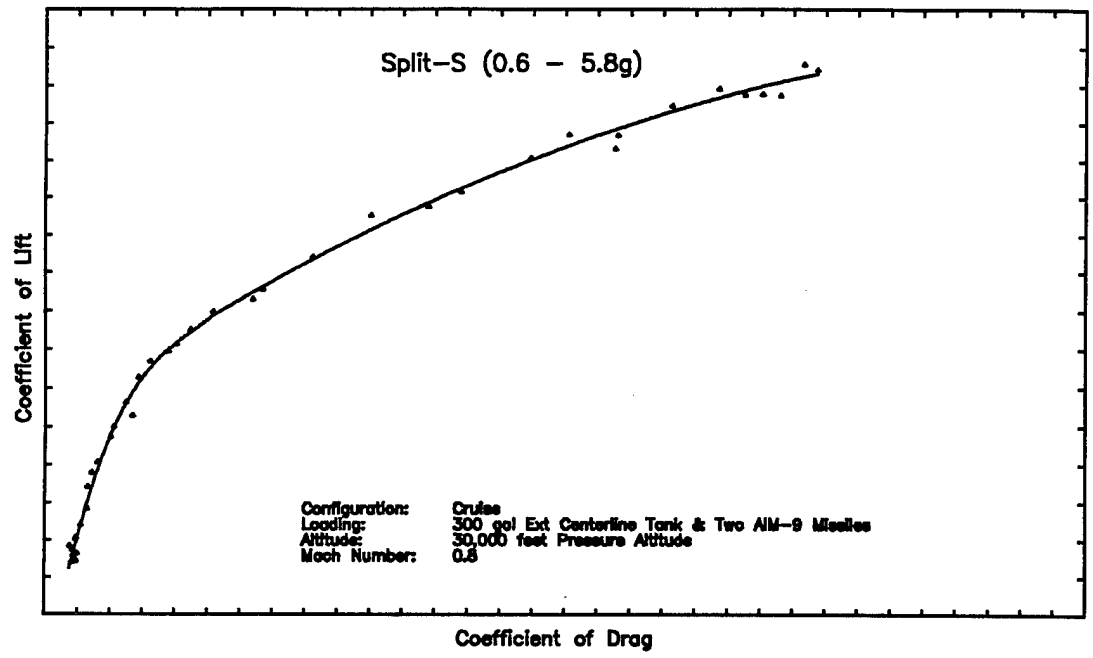

Figure 14.13 F-16B Drag Data obtained from a Split-S Maneuver

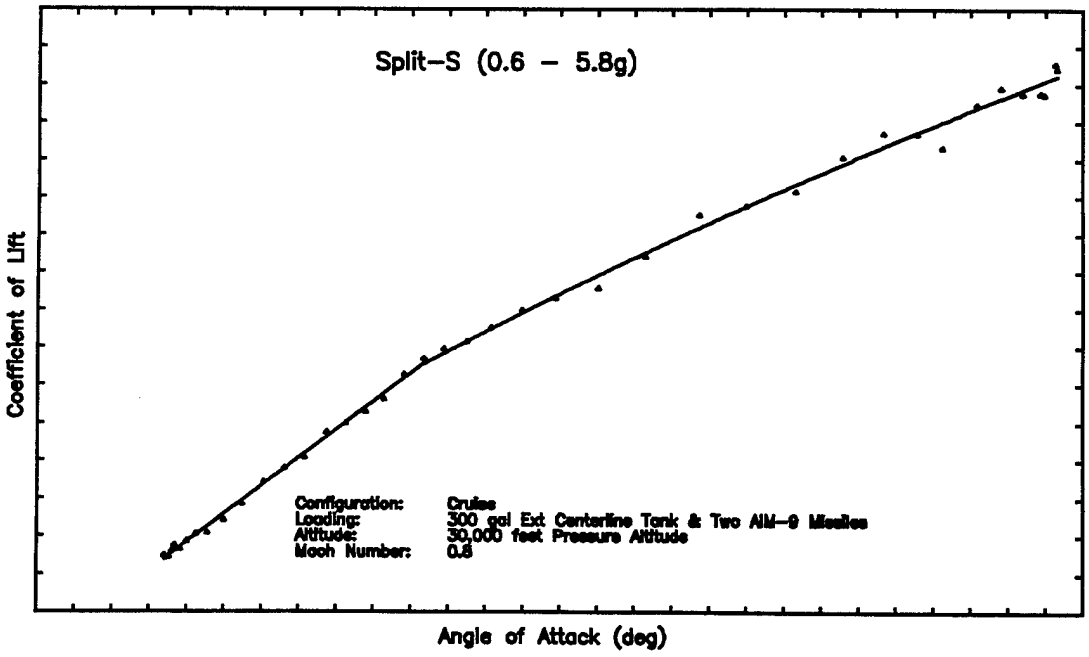

Figure 14.14 F-16B Lift Data obtained from a Split-S Maneuver

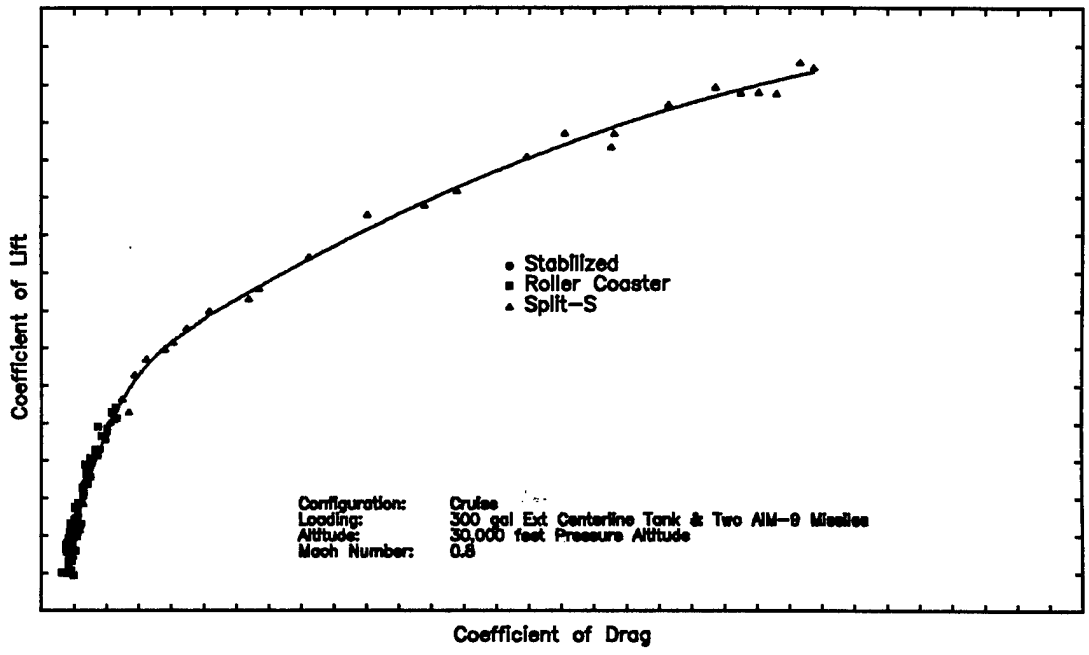

Figure 14.15 Comparison of F-16B Drag Data obtained from Stabilized, Roller Coaster, and Split-S Maneuvers

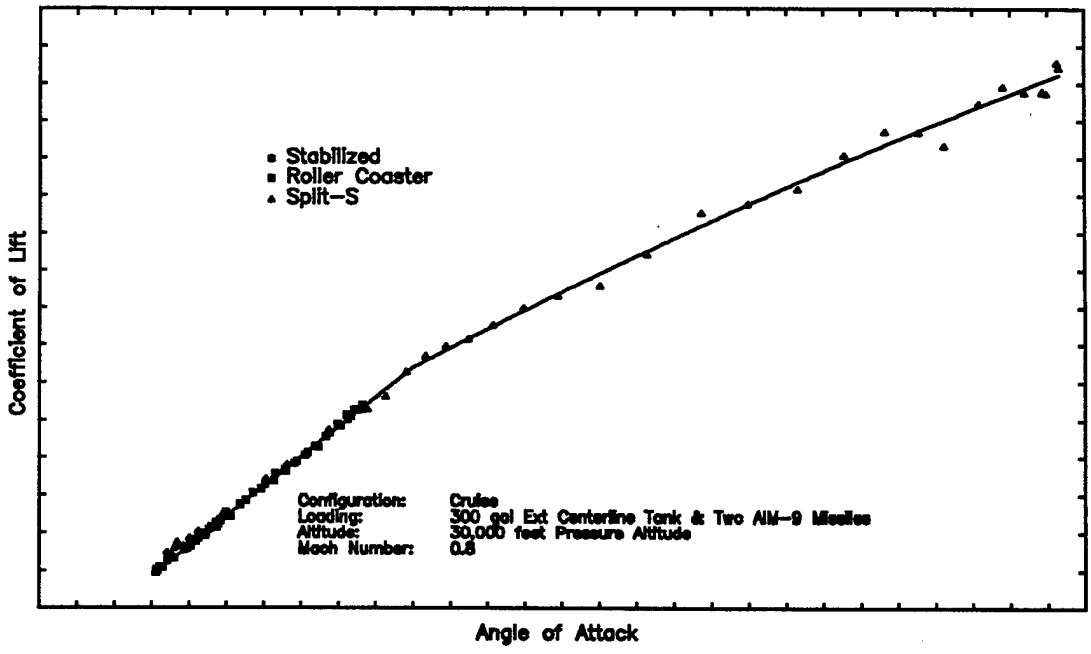

Figure 14.16 Comparison of F-16B Lift Data obtained from Stabilized, Roller Coaster, and Split-S Maneuvers

setting is used to control airspeed, pitch to control load factor, and bank angle to maintain constant altitude. The maneuver is first performed at wings level (1-g), then repeated at each desired load factor. Since the engine must be re-stabilized at each new load factor, this method takes the most time to set up. However, performed precisely, it can produce very accurate results.

14.3.1.1.2 DESCENDING TURN

The descending turn method allows for data collection within a small altitude band (usually ±1000 of target altitude) during a constant descent maneuver. This maneuver requires that bank angle be used to maintain both a constant descent rate and Mach number, with throttle position held constant, while pitch is used to maintain the desired load factor. The aircraft is first stabilized wings level (1 g) at the target altitude and Mach number, as was done in the constant altitude method, with the engine setting noted. The aircraft is then taken to 2000 ft above the target altitude and re-stabilized at the same engine setting. The descending turn maneuver is then performed at the desired load factor. Once stabilized at a constant descent rate, data are collected during a 5-10 second period within the ±1000 ft altitude band. The maneuver is repeated for each additional load factor desired. Note that the higher the load factor, the greater the descent rate will be in order to maintain a constant Mach number. This maneuver is very difficult to perform due to the sensitivity of descent rate to changes in bank angle. Nevertheless, successful data collection is dependent on maintaining both Mach number and descent rate constant.

14.3.1.1.3 DATA ANALYSIS

The data analysis required for the stabilized methods is inherently simpler than the quasisteady-state or dynamic maneuvering methods because the stabilized methods allow the following assumptions:

(a) no vertical (excluding gravity) or flight path acceleration ($a_{z_I} = a_{x_s} = 0$)
(b) no sideslip (ß=0, therefore the stability and wind axes are aligned)
(c) no side force generators
(d) fixed thrust vector ($\sigma_T = 0$, $\gamma_T = i_T$)

14.3.1.1.3.1 Angle of Attack

If angle of attack was not available from the aircraft instrumentation it can be calculated using equation 13.14b, from the Equations of Motion (EOM) I text (Reference 2). Applying the assumption that ß=0, this equation yields:

$$\dot{H}_c \frac{T_a}{T_{a_{sp}}} = V_t \left[\sin\theta\cos\alpha - \cos\Phi\cos\theta\sin\alpha\right] \qquad (14.3)$$

where

$\dot{H}_c \equiv$ climb rate (from the aircraft air data sytem)

$V_t \equiv$ true airspeed

$\Phi \equiv$ roll angle

$\theta \equiv$ pitch angle

Equation 14.3 can be used to solve for α using an iterative method. Notice that the vertical wind component, V_{W_z}, was not included in the equation since the aircraft air data system measures climb rate relative to the air mass, not the ground.

14.3.1.1.3.2 Lift and Drag Coefficient

We can use equation 13.26b, derived from equation 13.25 in the EOM I text, to determine lift and drag. With our assumptions, this general equation can be written in terms of stability coordinate system accelerations:

$$m \begin{Bmatrix} 0 \\ a_y \\ a_z \end{Bmatrix}_S = \begin{Bmatrix} -W\,(s\theta\, c\alpha - c\Phi\, c\theta\, s\alpha) - D + F_g\, c(\alpha + i_T) - F_e \\ W\, s\Phi\, c\theta \\ W\,(s\theta\, s\alpha + c\Phi\, c\theta\, c\alpha) - L - F_g\, s(\alpha + i_T) \end{Bmatrix}_S$$

where

a_{y_s} ≡ inertial acceleration in the y-stability (or wind) direction

a_{z_s} ≡ inertial acceleration in the z-stability (or wind) direction

F_g ≡ gross thrust

F_e ≡ engine drag

D ≡ aerodynamic drag

L ≡ aerodynamic lift

m ≡ mass

W ≡ weight

i_T ≡ angle of thrust

Note: $c \equiv \cos$, $s \equiv \sin$

The gross thrust and engine drag needed for this equation can be obtained from an engine model based on the required engine settings, Mach number, pressure altitude, and ambient temperature. Resolving the x-component of this equation produces the following equation for drag:

$$D = W\,(\cos\Phi\cos\theta\sin\alpha - \sin\theta\cos\alpha) + F_g\cos(\alpha + i_T) - F_e \qquad (14.4)$$

Without inertial acceleration measurements, the z-component of the general equation cannot be solved. However, if we rewrite EOM I equation 13.25 in terms of inertial coordinates and assume the z-acceleration is zero, we find the following expression for lift which is independent of the x and y accelerations:

$$m \begin{Bmatrix} a_x \\ a_y \\ 0 \end{Bmatrix}_I = \begin{Bmatrix} 0 \\ 0 \\ W \end{Bmatrix}_I + T^{IS} \begin{Bmatrix} -F_e - D \\ 0 \\ -L \end{Bmatrix}_S + T^{IB} \begin{Bmatrix} F_g \cos i_T \\ 0 \\ -F_g \sin i_T \end{Bmatrix}_B$$

The z-component of this relation produces the desired equation for lift:

$$L = \left\{ \frac{W - (F_e + D)\ (c\Phi\, c\theta\, s\alpha - s\theta\, c\alpha) - F_g\,(c\Phi\, c\theta\, s i_T + s\theta\, c i_T)}{(c\Phi\, c\theta\, c\alpha + s\theta\, s\alpha)} \right\} \tag{14.5}$$

Notice that both equations 14.4 and 14.5 simplify to classical lift and drag equations for the case of wings level flight ($\Phi = 0$):

$$D = -W \sin\gamma + F_g \cos(\alpha + i_T) - F_e \tag{14.4a}$$

$$L = \frac{W + (F_e + D)\sin\gamma - F_g \sin(\theta + i_T)}{\cos\gamma} \tag{14.5a}$$

The lift and drag coefficients can now be found from the following equations:

$$C_L = \frac{L}{qS} \tag{14.6a}$$

$$C_D = \frac{D}{qS} \tag{14.6b}$$

where

$$q \equiv \text{dynamic pressure} = \frac{1}{2}\rho_a V_t^2 = \frac{1}{2}\gamma P_{a_{SL}} \delta M^2$$

$$= 1481.36\ \text{lb/ft}^2\ \delta M^2 \tag{14.6c}$$

and

S ≡ reference wing area (ft^2)

$P_{a_{SL}}$ ≡ ambient pressure at sea level (= 2116.2 lb/ft^2)

γ ≡ 1.401 (air @ 40°F or 4°C)

M ≡ Mach number

δ ≡ pressure ratio, $\dfrac{P_a}{P_{a_{SL}}}$

14.3.1.2 QUASISTEADY-STATE METHODS

14.3.1.2.1 METHOD DESCRIPTION

The quasisteady-state method provides a means of collecting lift and drag data for a subsonic aircraft during constant altitude acceleration or deceleration maneuvers (Reference 3) at the desired load factors. It is assumed that the aircraft aerodynamic characteristics are not influenced by Mach number effects. The aircraft must be equipped with an inertial navigation unit (INU) or body accelerometer so that accelerations can be measured from a source other than the aircraft air data system, since, during an acceleration or deceleration maneuver, pneumatic line lags in the pitot static system can degrade the accuracy of the data collected. Additionally, the aircraft should be equipped with a data acquisition system so that data can be obtained at a rate of at least 2 samples per second. Aircraft equipped with an INU are initially stabilized at the desired initial speed and target altitude to allow for the calculation of wind velocity. These data will then be used for data reduction of quasisteady-state portion of the maneuver. Data required for the calculation of angle of attack, lift coefficient and drag coefficient include INU inertial velocities or body accelerometer measurements, calibrated airspeed, pressure altitude, ambient temperature, roll angle, pitch angle, yaw angle, angle of attack (if available), and the engine parameters necessary for thrust determination (C-23: Output shaft torque, τ_s, and propeller speed, N_p; C-141: engine pressure ratio, EPR; F-15, F-16, or T-38: engine core speed, N_2).

14.3.1.2.2 DATA ANALYSIS

The data analysis for the quasisteady-state methods requires the use of the aircraft velocity and force equations in their generalized form. The data analysis presented includes the following assumptions:

(a) zero sideslip during pre-maneuver stable point (ß=0, therefore the stability and wind axes are aligned)
(b) fixed thrust vector ($\sigma_T = 0$, $\gamma_T = i_T$)

14.3.1.2.2.1 Wind Velocity

For aircraft not equipped with an INU, the wind velocities should be obtained from a pacer aircraft so equipped or from weather balloon data. Otherwise, they must be assumed negligible. For aircraft equipped with an INU, the wind velocity can be directly computed from the INU velocities and the true airspeed calculated from the air data system measurements during stabilized flight prior to maneuvering. From equation 13.11 of the Equations of Motion I text:

$$\begin{Bmatrix} V_{W_x} \\ V_{W_y} \\ V_{W_z} \end{Bmatrix}_I = \begin{Bmatrix} V_x \\ V_y \\ V_z \end{Bmatrix}_I - T^{IW} \begin{Bmatrix} V_t \\ 0 \\ 0 \end{Bmatrix}_W$$

Wind Velocity | INU Velocity | Air Data System True Velocity

or

$$\begin{Bmatrix} V_{W_x} \\ V_{W_y} \\ V_{W_z} \end{Bmatrix} = \begin{Bmatrix} V_{x_I} - V_t [c\theta\, c\Psi\, c\alpha + (c\Phi\, s\theta\, c\Psi + s\Phi\, s\Psi)\, s\alpha] \\ V_{y_I} - V_t [c\theta\, s\Psi\, c\alpha + (c\Phi\, s\theta\, s\Psi - s\Phi\, c\Psi)\, s\alpha] \\ V_{z_I} - V_t [-s\theta\, c\alpha + c\Phi\, c\theta\, s\alpha] \end{Bmatrix} \tag{14.7}$$

where

V_{W_x} ≡ inertial x-component of wind

V_{W_y} ≡ inertial y-component of wind

V_{W_z} ≡ inertial z-component of wind

V_{x_I} ≡ INU inertial velocity component in x direction

V_{y_I} ≡ INU inertial velocity component in y direction

V_{z_I} ≡ INU inertial velocity component in z direction

V_t ≡ true airspeed

Ψ ≡ yaw angle

θ ≡ pitch angle

Φ ≡ roll angle

α ≡ angle of attack

The flight test noseboom measurements of α are used in the above equation. Otherwise, the assumption of $\alpha = \theta$ can be made, since the maneuver is accomplished during constant altitude, wings level flight. Once the winds are computed, the INU velocity relative to the air mass can be calculated at each data sample taken during the maneuver using the equation:

$$\begin{Bmatrix} V_{t_x} \\ V_{t_y} \\ V_{t_z} \end{Bmatrix}_I = \begin{Bmatrix} V_x \\ V_y \\ V_z \end{Bmatrix}_I - \begin{Bmatrix} V_{W_x} \\ V_{W_y} \\ V_{W_z} \end{Bmatrix}_I \tag{14.8}$$

INU velocity relative to air mass | **INU velocity** | **wind velocity**

14.3.1.2.2.2 Angle of Attack/Angle of Sideslip

The aircraft angle of attack and sideslip can either be measured in flight by use of special instrumentation, or if an INU is present, calculated using the INU velocities relative to the air mass through the relations derived with the help of Figure 14.17. From the figure we find

$$\alpha = \tan^{-1}\left(\frac{V_{t_{zB}}}{V_{t_{xB}}}\right) \tag{14.9}$$

$$\beta = \tan^{-1}\left(\frac{V_{t_{yB}}}{\sqrt{V_{t_{xB}}^{\ 2} + V_{t_{zB}}^{\ 2}}}\right) \tag{14.10}$$

and the flight path angle relative to the air mass, γ

$$\gamma = \tan^{-1}\left(\frac{-V_{t_{zI}}}{\sqrt{V_{t_{xI}}^{\ 2} + V_{t_{yI}}^{\ 2}}}\right) \tag{14.11}$$

where

$$\begin{Bmatrix} V_{t_x} \\ V_{t_y} \\ V_{t_z} \end{Bmatrix}_B = T^{BI} \begin{Bmatrix} V_{t_x} \\ V_{t_y} \\ V_{t_z} \end{Bmatrix}_I$$

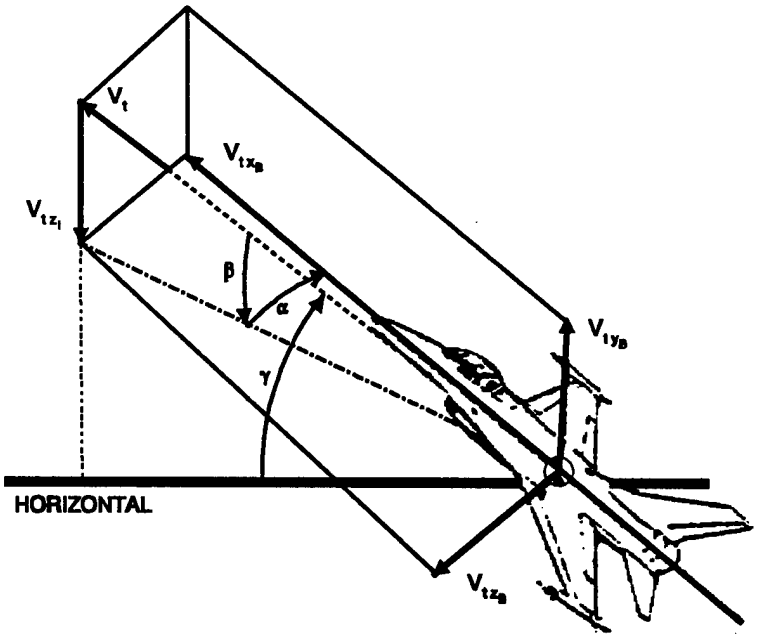

Figure 14.17 Calculation of α, β, and γ from the Components of INU True Airspeed

or

$$\begin{Bmatrix} V_{t_x} \\ V_{t_y} \\ V_{t_z} \end{Bmatrix}_B = \begin{Bmatrix} V_{t_{xI}} c\theta\, c\Psi + V_{t_{yI}} c\theta\, s\Psi - V_{t_{zI}} s\theta \\ V_{t_{xI}} (s\Phi s\theta\, c\Psi - c\Phi s\Psi) \\ + V_{t_{yI}} (s\Phi s\theta\, s\Psi + c\Phi c\Psi) \\ + V_{t_{zI}} s\Phi c\theta \\ V_{t_{xI}} (c\Phi s\theta\, c\Psi + s\Phi s\Psi) \\ + V_{t_{yI}} (c\Phi s\theta\, s\Psi - s\Phi c\Psi) \\ + V_{t_{zI}} c\Phi c\theta \end{Bmatrix}_B \qquad (14.12)$$

14.3.1.2.2.3 Lift and Drag Coefficients

Rewriting the left hand side of equation 13.26b of the EOM I text for body-axes accelerations, the general form of the force equation can be expressed as:

$$m\, T^{SB} \begin{Bmatrix} a_x \\ a_y \\ a_z \end{Bmatrix}_B = \begin{Bmatrix} -W (s\theta\, c\alpha - c\Phi c\theta\, s\alpha) - D - F_e + F_g\, c(\alpha + i_T) \\ W s\Phi c\theta + Y_A \\ W (s\theta\, s\alpha + c\Phi c\theta\, c\alpha) - L - F_g \sin(\alpha + i_T) \end{Bmatrix}_S$$

where

a_{x_B} ≡ inertial acceleration in the x-body direction
a_{y_B} ≡ inertial acceleration in the y-body direction
a_{z_B} ≡ inertial acceleration in the z-body direction
F_g ≡ gross thrust
F_e ≡ engine drag
D ≡ aerodynamic drag
L ≡ aerodynamic lift
m ≡ aircraft instantaneous mass
W ≡ aircraft instantaneous weight (= $m\, g_{SL}$)
g_{SL} ≡ sea level gravitational acceleration (= 32.174 ft/s^2)
i_T ≡ angle of thrust

The x-component of this equation provides an independent expression for aerodynamic drag:

$$D = F_g \cos(\alpha + i_T) - F_e - \frac{W}{g_{SL}} (a_{x_B} \cos\alpha + a_{z_B} \sin\alpha) - W (\sin\theta \cos\alpha - \cos\Phi \cos\theta \sin\alpha) \qquad (14.13)$$

The y-component provides an independent expression for aerodynamic side force:

$$Y_A = \frac{W}{g_{SL}} a_{y_s} - W \sin\Phi \cos\theta \tag{14.14}$$

And finally, the z-component produces an independent expression for aerodynamic lift:

$$L = - F_g \sin(\alpha + i_T) + \frac{W}{g_{SL}} (a_{x_s} \sin\alpha - a_{z_s} \cos\alpha) + W (\sin\theta \sin\alpha + \cos\Phi \cos\theta \cos\alpha) \tag{14.15}$$

The above equations are valid if the accelerations do not include gravitational acceleration. This would be the case if we calculated the accelerations by taking the time derivative of the INS inertial velocities. *However, if gravitational acceleration is included, as is true for body accelerometer measurements, the last term in each of the above equations is not needed.* For this case, the lift, side force, and drag equations are

$$D = F_g \cos(\alpha + i_T) - F_e - \frac{W}{g_{SL}} (a_{x_s} \cos\alpha + a_{z_s} \sin\alpha) \tag{14.13a}$$

$$Y_A = \frac{W}{g_{SL}} a_{y_s} \tag{14.14a}$$

$$L = - F_g \sin(\alpha + i_T) + \frac{W}{g_{SL}} (a_{x_s} \sin\alpha - a_{z_s} \cos\alpha) \tag{14.15a}$$

Obtaining gross thrust and engine drag from our engine model, the above equations can be solved. The lift and drag coefficients can then be found from equations 14.6a and 14.6b, while the side force coefficient, C_Y, can be found through the following similar expression:

$$C_Y = \frac{Y_A}{\bar{q}S} \tag{14.6d}$$

14.3.1.3 DYNAMIC METHODS

Dynamic methods provide a means of collecting lift and drag data at near constant Mach number over a large range of lift coefficients in a single maneuver (Reference 1). This is accomplished by varying load factor in a short period of time, with maneuvers lasting less than 10 seconds. The three maneuvers currently used in dynamic performance testing include the roller coaster, windup turn, and split-S. Each maneuver begins with a stabilized trim point to allow the engine to adequately stabilize and to collect data for calculating winds for use in reduction of the dynamic portion of the maneuver. It also provides a stabilized method "check" point for the

drag polar and lift curve developed. The aircraft must be instrumented with either a body accelerometer or inertial navigation unit (INU) and must be equipped with a data acquisition system (DAS) to collect data at a rate of at least 10 samples per second. Data required for the calculation of angle of attack, lift coefficient and drag coefficient include INU inertial velocities or body accelerometer measurements, calibrated airspeed, pressure altitude, ambient temperature, roll angle, pitch angle, yaw angle, angle of attack (if an INS is not available), and the engine parameters necessary for thrust determination (C-141A: engine pressure ratio, EPR; F-15, F-16, or T-38: engine core speed, N_2).

14.3.1.3.1 ROLLER COASTER (PUSHOVER-PULLUP)

The roller coaster maneuver consists of a smooth near-sinusoidal variation of load factor with time. The maneuver begins with a stabilized trim point at the target Mach number and altitude (N_z = 1 g). Once initially stabilized for 10 seconds, the maneuver progresses with a pushover to a load factor of less than 1 g. For fighter aircraft, this load factor is usually 0 g, while for transport aircraft, the load factor is only reduced to approximately 0.5 g. Note that throttle settings remain constant throughout the maneuver. The next step of the maneuver includes a pullup back through the initial 1 g load factor up to 1.5 g in transport aircraft or 2 g or more (or aim angle of attack) in fighter aircraft. Some Mach loss will occur at this point since the aircraft is at a higher drag condition with a positive flight path angle. The last step of the maneuver is a pushover back to a load factor of 1 g. The rate of change in load factor (or g onset rate) during the maneuver should be fast enough to maintain the Mach number within ±0.01 of the desired value. However, keeping this change below 0.5 g per second will help minimize dynamic effects. An entry technique adopted for fighter aircraft which will aid in this includes preceding the dynamic portion of the maneuver with a setup pushover-pullup maneuver to place the aircraft in a slight climb at the target Mach number.

14.3.1.3.2 WINDUP TURN

The windup turn maneuver consists of a smooth increase in load factor using bank angle to maintain Mach number constant. The aircraft is placed in a descending turn with pitch used to vary load factor from 1 to maximum g or angle of attack. The maneuver begins with a stabilized trim point at the target Mach number and the target altitude plus one half of the actual altitude loss expected during data collection. This increase in altitude is necessary to center the maneuver around the target altitude, and is generally around 1000 ft. Following the trim point, the aircraft is

gradually pulled into a descending turn with the load factor increasing at a rate of up to 1 g per second, up to maximum g or the angle of attack limit. This usually takes from 3 to 8 seconds depending on the aircraft type and pilot technique. Throttle setting remains constant throughout the maneuver to keep the engine stabilized and Mach number is maintained to within ± 0.01 of the target. The total altitude loss from the beginning of the maneuver to the end of recovery can be up to 10,000 ft, since the aircraft ends up pointing nearly straight down at the conclusion of the maneuver. While the wind-up turn can be utilized for nearly any aircraft, fighter aircraft should perform a pure inverted pullup (split-s) instead to obtain smoother data for the same range of lift coefficient, since roll rate effects are eliminated.

14.3.1.3.3 SPLIT-S (INVERTED PULLUP)

The third dynamic performance maneuver is performed similarly to that done during the initial part of a split-S maneuver. The maneuver begins with a stabilized trim point at the aim Mach number and the target altitude plus one half of the altitude loss expected during data collection. Again, as with the windup turn, this altitude increase allows the maneuver to be centered at the target altitude, and is generally between 500 and 1000 ft. Following the trim point, the aircraft is rolled inverted. After a momentary pause to allow roll and yaw to stabilize, an inverted pullup is flown at a rate of approximately 1-2 g per second, up to the maximum load factor or angle of attack. This usually takes between 3 to 5 seconds, depending on aircraft type and pilot technique. No attempt is made to minimize the Mach number variation, unless it exceeds ±0.01 during the data portion of the maneuver. If this occurs, the g onset rate must be increased, as required. The maximum load factor should be reached before 70° of pitch is exceeded. This will avoid getting data near 90° where some of the data reduction equations develop singularities and the aircraft INU transitions. Throttle setting is kept constant throughout the maneuver to maintain stable engine parameters. From the beginning of the maneuver to the end of recovery an altitude loss of over 10,000 ft can occur, depending on the test Mach number.

14.3.1.3.4 DATA ANALYSIS

The data analysis for the dynamic methods is identical to that presented for the quasisteady-state methods. However, INU data collected during a dynamic maneuver must be corrected, as discussed in section 14.4, before use in these equations. Additionally, during a dynamic maneuver, flight test nosebooms bend due to the high loading, causing errors in the value of angle of attack and angle of sideslip measured. Therefore, these angles should be calculated from INU data. For aircraft not equipped

with an INU, these errors can be corrected using contractor noseboom bending correction data, if available. Otherwise, these errors can be ignored with some loss in accuracy. Note that the equations presented previously included bank angle, making them valid for all three dynamic maneuvers.

14.3.2 AERODYNAMIC CHARACTERIZATION WITHOUT THE AID OF ENGINE MODELS

Two methods of determining lift and drag characteristics for an aircraft without the use of an engine model are presented. They include the asymmetric power technique and the mass consumption acceleration (MCA) method. The asymmetric power technique is a stabilized method involving an engine shut down. The MCA method uses quasisteady-state techniques (level accelerations and decelerations) to collect data to develop thrust and aerodynamic models.

14.3.2.1 ASYMMETRIC POWER TECHNIQUE

14.3.2.1.1 METHOD DESCRIPTION

The asymmetric power technique involves a series of constant airspeed stable point pairs performed throughout the aircraft airspeed envelope and operating weight to provide a variety of lift coefficients (Reference 4). The stable point pairs include a constant altitude stable point with all engines operating, followed by a constant descent stable point with one engine shut down. This method assumes that each engine provides an equal amount of thrust. The test technique begins by stabilizing the aircraft at the test altitude and airspeed with all engines set at the same power setting. Once stabilized, data are recorded, including the current power setting. The aircraft is then flown to approximately 1000 ft above the test altitude and re-stabilized at the original power setting and test airspeed. One engine is shut down, and, if propeller driven, the propeller is feathered. On aircraft with three or more engines, the shut down engine should be the center or most inboard engine to minimize additional trim drag. The aircraft is then placed into a descent, as required, to maintain the aim airspeed. As the aircraft descends through the test altitude, descent rate is measured and recorded. For propeller aircraft, this method assumes that trim drag, feathered propeller drag, cooling drag increments, and the slipstream drag increments are partially cancelling and can be assumed zero. However, for turbo prop and turbo fan aircraft, while the additional trim drag during the stable descent is assumed negligible, the ram drag of the shut down engine cannot be ignored. Obviously, with the assumptions stated, this method is less accurate than those presented for use with the aid of engine models. The data required for post-flight analysis of asymmetric power test points include pressure altitude, calibrated

airspeed, ambient temperature, climb rate, pitch angle, engine speed (for shut down engine), and angle of attack, if available, for both the constant altitude and constant descent rate stable points.

14.3.2.1.2 DATA ANALYSIS

The assumptions, other than those previously stated, include:

(a) zero sideslip (ß = 0)
(b) zero roll (Φ = 0)
(c) zero acceleration (excluding gravity)
(d) lift coefficient/angle of attack variation between constant altitude and constant descent points is insignificant

14.3.2.1.2.1 Flight Path Angle/Angle of Attack

Rearranging equation 13.14b from the EOM I text and applying the assumptions presented produces:

$$\dot{H}_c = \left(\frac{T_{a_{sp}}}{T_a}\right) V_t \sin(\theta - \alpha) = \left(\frac{T_{a_{sp}}}{T_a}\right) V_t \sin\gamma \qquad (14.16)$$

where

$\dot{H}_c$ ≡ climb rate
V_t ≡ true airspeed
T_a ≡ ambient temperature
$T_{a_{SD}}$ ≡ standard day ambient temperature at test altitude
θ ≡ pitch angle
α ≡ angle of attack
γ ≡ flight path angle (= θ - α)

Solving for α:

$$\alpha = \theta - \sin^{-1}\left(\frac{\dot{H}_c\ T_a}{V_t\ T_{a_{sp}}}\right) \qquad (14.17)$$

For the engine-out stabilized descent, substituting and solving for γ, this equation yields

$$\gamma_{EO} = \sin^{-1}\left(\frac{\dot{H}_c\ T_a}{V_t\ T_{a_{sp}}}\right)_{EO} \qquad (14.17a)$$

The angle of attack can now be found using the measured pitch angle during the descent. Thus,

$$\alpha_{EO} = \theta_{EO} - \gamma_{EO} \qquad (14.17b)$$

During the constant altitude stable point with all engines operating, $\dot{H}_c = 0$. Therefore,

$$\gamma_{AE} = 0 \tag{14.17c}$$

and

$$\alpha_{AE} = \theta_{AE} \tag{14.17d}$$

14.3.2.1.2.2 Lift and Drag Coefficients

With our assumptions, equations 14.4a and 14.5a, derived for the stabilized methods, can be used to calculate lift and drag. *For the constant altitude stable point*, these equations simplify to:

$$D_{AE} = F_{n_{AE}} \tag{14.18}$$

and

$$L_{AE} = -F_{g_{AE}} \sin(\alpha_{AE} + i_T) + W \cong W \tag{14.19}$$

where

D_{AE} ≡ drag with all engines operating

$F_{n_{AE}}$ ≡ net thrust for all engines operating

$= F_{g_{AE}} \cos(\alpha_{AE} + i_T) - F_{e_{AE}}$

$F_{g_{AE}}$ ≡ total gross thrust for all engines operating

$F_{e_{AE}}$ ≡ total engine drag for all engines operating

Notice that equation 14.19 for lift made the assumption that the term *sin* $(\alpha+i_T)$ was small enough to be ignored, thus allowing for direct calculation of lift.

With thrust unknown in equation 14.18, let us now look at the corresponding *constant descent engine-out stable point.* For this case equations 14.4a and 14.5a produce:

$$D_{EO} = F_{n_{EO}} - W \sin\gamma_{EO} \tag{14.20a}$$

and

$$L_{EO} = \frac{W - (F_{g_{EO}} \sin(\alpha_{EO} + i_T) - F_{e_{EO}} - D_{EO}) \sin\gamma_{EO}}{\cos\gamma_{EO}} - F_{g_{EO}} \sin(\alpha_{EO} + i_T)$$

$$\cong \frac{W}{\cos\gamma_{EO}} - \left(F_{n_{EO}} - D_{EO}\right) \tan\gamma_{EO} \tag{14.21b}$$

where

D_{EO} ≡ drag during engine-out descent

$F_{n_{EO}}$ ≡ net thrust during engine-out descent

Again, we assumed the term *sin* $(\alpha+i_T)$ was small enough to be ignored in the lift equation, eliminating the second term. Now if we assume that the difference in thrust between all engines operating and with an engine out is

$$F_{n_{AE}} - F_{n_{EO}} = \frac{F_{n_{AE}}}{N_{eng}} + F_{r_{SE}}$$

or

$$F_{n_{EO}} = \frac{(N_{eng}-1)\, F_{n_{AE}}}{N_{eng}} - F_{r_{SE}} \tag{14.22}$$

where

N_{eng} ≡ total number of engines

$F_{r_{SE}}$ ≡ single engine windmilling ram drag (obtained from engine manufacturers curves based on engine speed, altitude, and Mach number)

then equations 14.20a and 14.21a can be written as:

$$D_{EO} = \frac{(N_{eng}-1)\, F_{n_{AE}}}{N_{eng}} - F_{r_{SE}} - W \sin\gamma_{EO} \tag{14.20b}$$

and

$$L_{EO} = \frac{W}{\cos\gamma_{EO}} + \left\{ D_{EO} - \frac{(N_{eng}-1)\, F_{n_{AE}}}{N_{eng}} \right\} \tan\gamma_{EO} \tag{14.21b}$$

With the variation in lift coefficient between all engines and engine-out stable points assumed negligible,

$$D_{EO} \equiv D_{AE} = D \tag{14.22}$$

And, with our assumption that all engines provide the same thrust, we can substitute equation 14.18 and the above equation into equation 14.20b to produce the desired equation for drag

$$D = -N_{eng} (F_{r_{SE}} + W \sin\gamma_{EO}) \tag{14.20c}$$

Using the same substitutions, the lift during the engine-out stable descent can then be calculated from

$$L_{EO} = \frac{W}{\cos\gamma_{EO}} + \left(\frac{D}{N_{eng}} \right) \tan\gamma_{EO} \tag{14.21c}$$

Now, equation 14.6a can be used to calculate the drag coefficient. We can then use equation 14.6b to calculate the lift coefficients for the constant altitude and constant descent stable points based on the lift calculated from equations 14.19 and 14.21b, respectively. Comparison of these lift coefficients will allow us to determine if our original assumption assuming insignificant variation in lift coefficient was valid.

14.3.2.2 MASS CONSUMPTION ACCELERATION METHOD

The MCA method is a flight test technique developed by the German Flight Test Center to determine the in-flight thrust and drag characteristics of an aircraft without the use of a separate propulsion model. Instead the flight-mechanical dynamics of the total aircraft system are used to develop an integrated thrust and drag model. The method is based on the principle of the conservation of energy - in particular the conversion of thermal energy (fuel) into mechanical energy (kinetic) - and uses the overall aircraft efficiency as a variable in the determination of in-flight thrust. Since the method considers the aircraft as a whole, including the engine, the normal distinction between the engine and fuselage cannot be made. The flight testing required to support this method includes a series of wings level accelerations and decelerations at constant altitude and power setting over the speed range of the aircraft.

The advantage of the MCA method is that it requires very few, commonly available measurement parameters: aircraft mass, fuel flow, body accelerations and orientation, true airspeed, and ambient conditions. The disadvantage is that the method requires a great deal of complex data reduction, as described in Reference 5. A discussion of this data reduction is beyond the scope of this course.

14.3.3 DATA STANDARDIZATION

Final standardization of flight test aerodynamic data requires the use of contractor aerodynamic models derived from wind tunnel or previous flight testing. For a given configuration and loading, aerodynamic data are standardized at the test lift coefficient, target Mach number, and standard conditions (standard center of gravity, standard altitude, etc), as appropriate for the particular model. The drag coefficient and angle of attack are standardized by adding corrections derived from the contractor model. Thus,

$$C_{D_{ST}} = C_D + \Delta C_{D_{ST}} \tag{14.23}$$

and

$$\alpha_{ST} = \alpha + \Delta\alpha_{ST} \tag{14.24}$$

The corrections are determined from the model predictions of test and standardized drag coefficient and angle of attack:

$$\Delta C_{D_{ST}} = C_{D_{ST_{pred}}} - C_{D_{pred}} \tag{14.25}$$

$$\Delta\alpha_{ST} = \alpha_{ST_{pred}} - \alpha_{pred} \tag{14.26}$$

14.4 INERTIAL NAVIGATION UNIT CORRECTIONS

Inertial navigation units (INUs) are self-contained systems that supply all data necessary in defining the motion of an aircraft in three-dimensional space. However, since it is usually not possible to locate this unit at the aircraft center of gravity (cg), the data must be corrected before being used in the air data computer or in data reduction routines (Reference 6).

14.4.1 FUSELAGE BENDING CORRECTIONS

Bending in the fuselage requires the correction of the three orientation angles measured by the INU. Generally, the only significant deflection in the fuselage occurs in the pitch axis. Since many INUs are located ahead of the cg, an upward load factor will cause the INU to be rotated below the normal x_B-axis by an angle σ_f, as shown in Figure 14.18. This deflection is a function of Mach number, load factor, dynamic pressure, angle of attack, and forward fuel weight, and it can be determined by analysis of the aircraft structural characteristics and pressure model tests in the wind tunnel.

Thus, once the deflection angle is calculated, the corrections to the measured platform angles can be found from the following equations:

$$\Psi_{INU} = \theta_y + \sigma_f \sin \theta_R \quad (14.27a)$$

$$\theta_{INU} = \theta_p + \sigma_f \cos \theta_R \quad (14.27b)$$

$$\Phi_{INU} = \theta_R \quad (14.27c)$$

where

$\theta_y \equiv$ platform yaw angle
$\theta_p \equiv$ platform pitch angle
$\theta_R \equiv$ platform roll angle

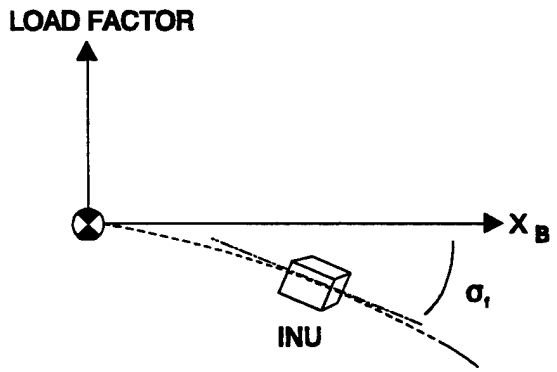

Figure 14.18 Fuselage Deflection

14.4.2 CENTER OF GRAVITY CORRECTIONS

Because the INU is located ahead of the cg, it senses additional accelerations and velocities induced by aircraft rotation that must be corrected for. If the location of the INU relative to the cg is known, the necessary corrections based on the corrected orientation angles can be determined.

Figure 14.19 provides a schematic of the INU location relative to the aircraft cg, where the x_B, y_B, and z_B distances are defined by l_x, l_y, l_z, respectively. From this figure we find that the corrections in the body-fixed reference frame velocities are given by

$$\Delta V_{x_B} = -Q l_z + R l_y \tag{14.28a}$$

$$\Delta V_{y_B} = -R l_x + P l_z \tag{14.28b}$$

$$\Delta V_{z_B} = -P l_y + Q l_x \tag{14.28c}$$

and the acceleration corrections:

$$\Delta a_{x_B} = \dot{R} l_y - \dot{Q} l_z + l_x (Q^2 + R^2) - P (Q l_y + R l_z) \tag{14.29a}$$

$$\Delta a_{y_B} = \dot{P} l_z - \dot{R} l_x + l_y (P^2 + R^2) - Q (R l_z + P l_x) \tag{14.29b}$$

$$\Delta a_{z_B} = \dot{Q} l_x - \dot{P} l_y + l_z (P^2 + Q^2) - R (P l_x + Q l_y) \tag{14.29c}$$

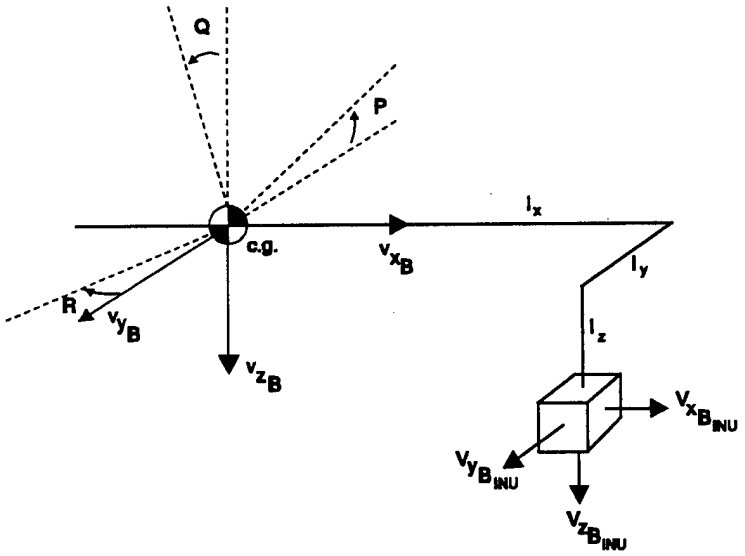

Figure 14.19 Inertial Measurement Unit Location Relative to Aircraft Center of Gravity

The inertial body system angular rates, P, Q, and R used in the above relations are determined from equations 13.16a, 13.16b, and 13.16c of the EOM I text. The angular accelerations, $\dot{P}$, $\dot{Q}$, and $\dot{R}$, are found from the time derivatives of these rates. Note that the platform angles must be corrected for fuselage bending (equations 14.27a, 14.27b, and 14.27c) before substitution into the angular rate equations.

Once the corrections due to aircraft rotation have been calculated, they can be added to the measured INU motion. However, care must be taken to ensure the proper transformations are first performed, keeping in mind that the above correction relations are defined in the *body axis*. The final inertial aircraft velocity and acceleration at the center of gravity expressed in the inertial frame can therefore be calculated from the following equations:

$$\begin{Bmatrix} V_x \\ V_y \\ V_z \end{Bmatrix}_I = T^{I\,INU} \begin{Bmatrix} V_{x_{meas}} \\ V_{y_{meas}} \\ V_{z_{meas}} \end{Bmatrix}_{INU} + T^{IB} \begin{Bmatrix} \Delta V_x \\ \Delta V_y \\ \Delta V_z \end{Bmatrix}_B \tag{14.30}$$

$$\begin{Bmatrix} a_x \\ a_y \\ a_z \end{Bmatrix}_I = T^{I\,INU} \begin{Bmatrix} a_{x_{meas}} \\ a_{y_{meas}} \\ a_{z_{meas}} \end{Bmatrix}_{INU} + T^{IB} \begin{Bmatrix} \Delta a_x \\ \Delta a_y \\ \Delta a_z \end{Bmatrix}_B \tag{14.31}$$

14.5 SUMMARY

In this chapter, the subject of aircraft aerodynamic modeling, with and without engine models, was presented. The flight test techniques discussed included stabilized, quasisteady-state, and dynamic methods, with the basic equations necessary for analysis of each provided in detail. An underlying goal was to develop an appreciation for the advantages and limitations offered by each flight test technique for application to future test programs.

(This page intentionally left blank)

14.6 REFERENCES

1. Olson, Wayne, Aircraft Performance Flight Testing Office Memo, January 1991.

2. Equations of Motion I, Chapter 13, Volume I, USAF Test Pilot School, July 1992.

3. Yechart, T.R., Flight-Test Determination of Aircraft Cruise Characteristics Using Acceleration and Deceleration Techniques, July 1988, J. Aircraft, Vol 25, No 7.

4. Roberts, Sean C., Light Aircraft Performance for Test Pilots and Flight Test Engineers, 9 July 82.

5. Rosenberg, Richard E., The MCA Method of Determining Thrust of a Jet Aircraft, AIAA Publication, 1985.

6. Olhausen, JN, Use of a Navigation Platform for Performance Instrumentation on the YF-16, Journal of Aircraft, Vol 13, No. 7, April 1976, pp. 231-237.

(This page intentionally left blank)